ACS Macro Letters

Letter

pubs.acs.org/macroletters

# Synthesis of Conducting Polymer–Metal Nanoparticle Hybrids Exploiting RAFT Polymerization

Paul E. Williams,[†] Samuel T. Jones,[†] Zarah Walsh, Eric A. Appel, Enass K. Abo-Hamed, and Oren A. Scherman*

Melville Laboratory for Polymer Synthesis, Department of Chemistry, University of Cambridge, Lensfield Road, Cambridge CB2 1EW, United Kingdom

Supporting Information

**ABSTRACT:** The direct covalent attachment of conducting polymers (CP) to nanoparticles (NP) to form CP-NP nanohybrids is of great interest for optoelectronic device applications. Hybrids formed by covalently anchoring CP to NP, rather than traditional blending or bilayer approaches, is highly desirable. CP-NP nanohybrids have increased interfacial surface area between the two components, facilitating rapid exciton diffusion at the *p*–*n* heterojunction. These materials take advantage of the facile solution processability, lightweight characteristics, flexibility, and mechanical strength associated with CPs, and the broad spectral absorption, photostability, and high charge carrier mobility of NPs. We demonstrate the ability to polymerize a hole transporting (HT) polymer utilizing reversible-addition–fragmentation chain transfer (RAFT) polymerization and its subsequent rapid aminolysis to yield a thiol-terminated HT polymer. Subsequent facile attachment to gold (Au) and silver (Ag) NPs and cadmium selenide (CdSe) quantum dots (QDs), to form a number of CP–NP systems is demonstrated and characterized. CP–NP nanohybrids show broad spectral absorptions ranging from UV through visible to the near IR, and their facile synthesis and purification could allow for large scale industrial applications.

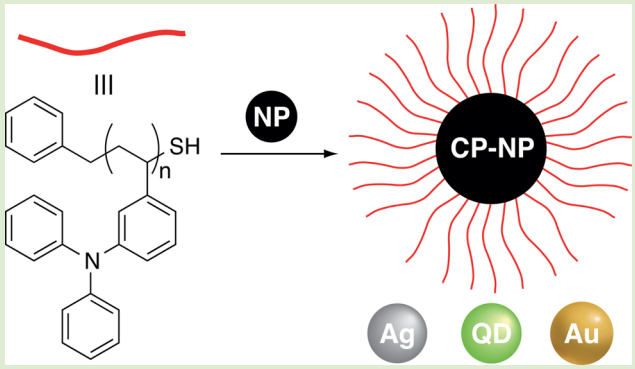


The direct covalent attachment of conducting polymers (CP) to nanoparticles (NP) to form CP–NP nanohybrids (where "–" indicates direct covalent attachment) is of great interest for optoelectronic device applications. CP–NP nanohybrids increase the interfacial surface area between the two components, facilitating rapid exciton diffusion at the *p*–*n* heterojunction, and take advantage of the inherent solution processability, flexibility, and mechanical strength associated with CPs, along with the broad spectral absorption, photostability, and high charge carrier mobility of NPs.[1−7] To prevent NPs from aggregating, leading to loss of their inherent optoelectronic properties, a sufficient surface coating of solubilizing ligands is paramount.[8,9] The use of conducting polymers as the solubilizing ligand opens up a range of potential applications in areas such as field-effect transistors (FETs), organic light emitting diodes (OLEDs) and photovoltaics. Through attachment in this manner a *p*–*n* heterojunction is created between a *p*-type hole transporting (HT) conducting polymer (CP) and a *n*-type electron transporting (ET) NP. Creating such a *p*–*n* heterojunction directly at the interface between CPs and NPs allows for the rapid charge separation of an exciton into corresponding holes and electrons,[10] on account of the fact that hole mobilities in organic CPs far exceed electron mobilities[11] and the electron affinities of inorganic NPs are generally greater.[1,10] Traditionally, there are two methods for integrating CPs and NPs, either blending or direct covalent attachment. Blending techniques give CP/NP nanohybrids (where "/" denotes physical blending) by either constructing a CP/NP bilayer or a CP/NP alternating multilayer.[12] In either case, blending of CPs and NPs leads to low quantum efficiencies (QE)[13] and device lifetimes on account of poor interfacial surface contacts between the two components,[1,13] macrophase separation and aggregation of NPs over time, and the presence of insulating ligands on the NP surface, which are not displaced during blending.[10,11,13] Better control over the morphology of the CP/NP nanohybrids and, subsequently, the *p*–*n* heterojunction is critical in ensuring an interpenetrated network of CPs and NPs on the order of the exciton diffusion length (ca. 5–10 nm).

Direct covalent tethering of CPs onto NPs allows for improved control over the hybrid morphology, giving rise to greater interfacial contacts between the two components, which is key to ensuring the optimization of the *p*–*n* heterojunctions.[14−16] The ability to chemically anchor the CP to the NP gives a controlled, uniform coating and displaces insulating ligands. Such an approach also prevents macrophase separation

**Received:** October 9, 2014
**Accepted:** January 23, 2015
**Published:** February 3, 2015





DOI: 10.1021/mz500645c
*ACS Macro Lett.* 2015, 4, 255–259

but facilitates nanophase separation at the $p-n$ heterojunction on the order of the exciton diffusion length.[17,18] Additionally, NPs also reduce the lifetime of triplet exciton states reducing photo-oxidation of CPs.[4] All of the above contribute greatly to enhanced charge transfer efficiencies and prolonged device lifetimes. CP−NP nanohybrids have been shown to have several orders of magnitude better conductivity than their analogous CP/NP counterparts.[4] Herein, we report the facile synthesis of a thiol-terminated HT *meta*-triphenylamine (*m*-TPA) homopolymer (**2**) by a controlled radical polymerization technique, followed by its subsequent attachment to gold (Au), silver (Ag), and cadmium selenide (CdSe) NPs, affording broad spectral absorbent, monodisperse, and well-defined CP−NP nanohybrids (Scheme 1).

**Scheme 1. Facile Functionalization of Au (3a), Ag (4a), and CdSe (5a) Nanoparticles (QD) with 2 to Form CP−NP Nanohybrids (3b, 4b, and 5b, respectively)**

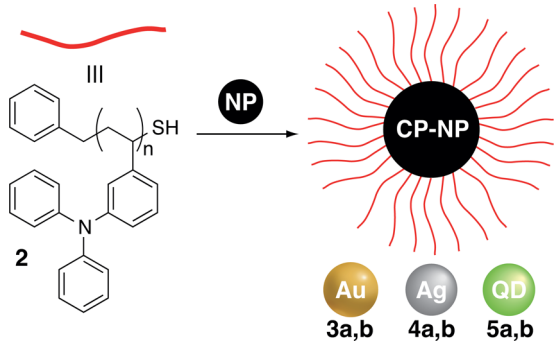


There are two classes of CP available for optoelectronic device applications, namely, main-chain and side-chain. Many reports investigating the direct tethering of main-chain CPs onto NPs have appeared in the literature and include ligand exchange,[11,19−25] direct growth from the NP surface,[4,8,13] electrostatic interactions,[26,27] or molecular recognition of hydrogen bonding motifs[28] to achieve CP−NP nanohybrids with controlled morphologies and charge transfer interfaces. Main-chain CPs have several fundamental advantages over side-chain CPs, including higher conductivity and better device efficiencies on account of chemical conjugation through the main polymer chain, rather than electron hopping through the side chain. Main-chain CPs, however, typically display poor solution processability, require difficult and complex synthetic routes, and harsh polymerization procedures (i.e., oxidative coupling), generally generating low MW polymers with high polydispersities (PDI), giving rise to ill-defined morphologies, which severely limit their scalability and thus their applicability.[29] Additionally, main-chain CPs may not possess an inherent functional end group for direct tethering to NPs, therefore, further complex chemistries are often necessary to functionalize main-chain CPs for covalent tethering that often utilize a nonconjugated linker resulting in poor exciton diffusion at the CP−NP interface.[4]

In this study, for the preparation of broad spectral absorbent CP−NP nanohybrids, thiol-terminated HT−CPs were first synthesized via reversible-addition−fragmentation chain transfer (RAFT) polymerization. RAFT is a controlled radical polymerization (CRP) technique that has recently been utilized for the synthesis of side chain conducting homopolymers and block copolymers containing one or more of the active components of optoelectronic devices.[30,31] Achieving monodisperse CPs is key to eliminating low molecular weight impurities, which can act as electron and hole traps.[31] Another major advantage of RAFT is the facile synthesis of chain transfer agents (CTA) allowing for a broad range of functionality[32,33] as well as affording the ability to modify the resulting polymers postpolymerization to achieve varied end-group functionality.[34,35] Importantly, reduction of the latent CTA leads to thiol-functional polymers, which in the presence of gold, silver, and platinum NPs can form organic−inorganic hybrid materials.[36] Preparation of **1** was achieved by the polymerization of *m*-TPA with the analogous CTA and AIBN in dioxane and the polymer was characterized by gel permeation chromatography (GPC) and nuclear magnetic resonance (NMR; Table S1). The HT−CP was obtained with a targeted degree of polymerization (DP) of 42 (PDI = 1.14), giving a polymer chain length coinciding with the exciton diffusion length (ca. 5−10 nm) in order to minimize recombination events.

In order to covalently attach HT−CP homopolymers to NPs to achieve a CP−NP nanohybrid, a thiol-terminated functional polymer was prepared from **1**. This was achieved by the fast aminolysis of a solution of **1** in DMF/THF with hydrazine,[37] a change in color, from yellow to colorless, was observed indicating the formation of **2** after 10 min. Thiol-terminated polymer (**2**) was calculated to have the same DP (42) as **1** but with a lower molecular weight (11.3 kDa) due to the loss of the Z group, showing that the aminolysis with hydrazine had occurred. The reaction was also confirmed by GPC analysis, which showed that there had been a slight decrease in molecular weight (ca. 7.0 kDa for **1** and 6.7 kDa for **2**) indicative of Z group loss and is consistent with NMR interpretation, with only a slight broadening in PDI ($\delta_{ppm}$ = 1.14 for **1** and 1.19 for **2**; Table S1). The slight broadening in PDI can be accounted for by comparing GPC traces of **1** and **2**; the trace for **2** contained a small high molecular weight shoulder, which is characteristic of disulfide coupling between thiols (see Supporting Information). The presence of disulfides is insignificant and has no effect on the system as it has been demonstrated that disulfides still react with NPs in a similar fashion as free thiols.[38]

Au (**3a**) and Ag (**4a**) NPs were synthesized yielding NPs that were soluble in toluene,[39] a good solvent for **2**, and stabilized with dodecylamine ligands. Thiol groups are well-known to bind strongly to both Au and Ag NPs and can easily replace the dodecylamine ligands. NPs with a diameter of ∼5 nm were selected as this size offers a high degree of curvature allowing for maximum surface coverage of **2** and maximum exposure of the CP to the solution.[40] Moreover, the size of NPs directly determines their absorption and emission properties, which are typically tuned to range from ultraviolet (UV), through visible (vis), to near-infrared (IR).[10,41−44] These NPs also have broad spectral absorbances within the visible region making them great candidates as exciton sources for optoelectronic applications, as well as being on the same order as the exciton diffusion length. The metal NPs were simply mixed with **2** in solution and resulted in complete functionalization after ∼48 h. Excess **2** and dodecylamine were readily removed by a hexane wash followed by centrifugation. This procedure was repeated twice more to yield **3b** and **4b**. CdSe NPs (**5a**) of a similar size and solubility to **3a** and **4a** were donated.[45] Like metal NPs, CdSe NPs have been shown to react with thiols, allowing for **5b**


DOI: 10.1021/mz500645c
ACS Macro Lett. 2015, 4, 255−259

to be prepared from **5a** using the same functionalization procedure as above, highlighting the versatility of this method.

To fully characterize the formed CP−NP nanohybrids, several techniques were used, including thermogravimetric analysis (TGA), dynamic light scattering (DLS), solution phase UV−vis spectroscopy, atomic force microscopy (AFM), transmission electron microscopy (TEM), and for the first time to the authors' knowledge for such CP−NP nanohybrids, GPC. Analysis of **2** by UV−vis spectroscopy reveals a strong absorbance in the UV region centered at 300 nm (see Supporting Information), while 5 nm Au and AgNPs (**3a** and **4a**) have absorbances centered at 521 and 421 nm, respectively, with CdSe NPs **5a** absorbing at 635 nm. The spectra of the prepared CP−NP nanohybrids revealed no change in the characteristic absorbances of any of the components of the hybrid systems, showing that functionalization was achieved without causing aggregation or altering the NP size or shape. A full UV−vis spectrum of each system (**3b**, **4b**, and **5b**; Figure 1a) highlights the inherent broad spectral absorbances, which

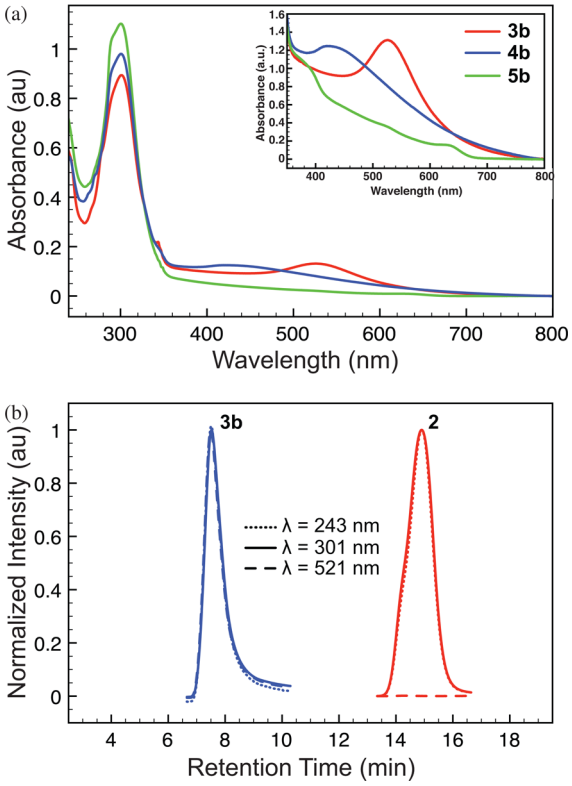


**Figure 1.** (a) UV−vis spectroscopy of CP−NP nanohybrids **3b**, **4b**, and **5b**. (b) GPC analyses of thiol-functional polymer **2** and CP−NP nanohybrid **3b** in THF. There is a perfect overlay of the absorbance from the polymer ($\lambda_{max}$ = 243 and 301) and the NP ($\lambda_{max}$ = 521) in CP−NP nanohybrid **3b**, supporting covalent conjugation of the polymer to the NP.

range from the UV through visible to near IR (ca. 200−650 nm) making them potentially intriguing materials for optoelectronic device applications.

UV−vis spectroscopy, however, does not confirm the direct attachment of **2** to the NPs, therefore, GPC in isocratic elution mode over 40 min in THF was performed on all samples. Resulting chromatograms clearly show that a lower retention time is observed for **3b** (8 min) when compared to **2** (14 min; Figure 1b). Shorter retention times indicate a large hydrodynamic volume, and likely a higher MW, thereby indicating **3b** is a composite of **2** and **3a**. This is further verified from the UV signal showing that the characteristic absorbance at 521 nm for Au-NPs is clearly present after functionalization of **3a** with **2** (blue trace), along with the absorbances for **2** ($\lambda_{max}$ = 243 and 301 nm), indicating that a complete coating of **3a** with **2** had occurred and that no free polymer remained. UV traces of polymer **2** (red trace) show only absorbances characteristic of **2** ($\lambda_{max}$ = 243 and 301 nm) with no absorbance for Au-NP ($\lambda_{max}$ = 521 nm).

Determining the surface coverage of **2** on the NPs is important to understand the potential properties of the CP−NP nanohybrids relating to the distribution of the *p*−*n* heterojunctions. TGA is a commonly utilized technique for characterizing the surface coverage of functionalized NPs by analyzing the mass loss at $T_{onset}$ relative to the remaining mass. TGA analysis of **2** showed complete mass loss at $T_{onset}$ > 400 °C. When **3b** was analyzed using TGA a mass loss of 66% was observed at $T_{onset}$ > 400 °C accounting for the loss of polymer, the remaining mass can be attributed to Au-NPs, which have thermal stabilities at temperatures greater than 500 °C (Figure S3b). Knowing the MW of both **2** (10.7 kDa) and **3a** (calculated to be ∼1000 kDa), the percentage weight loss data obtained from TGA analyses showed that **3b** consisted of approximately 110 polymer chains (**2**) per AuNP (**3a**).

To corroborate the data obtained from GPC analysis of CP-NP nanohybrid systems, DLS was conducted on the nanohybrids pre- and postfunctionalization. It was observed that the hydrodynamic diameter ($d_h$) in each case increased upon functionalization of the NPs with **2**: Au ($\Delta d_h$ = 6 nm), Ag ($\Delta d_h$ = 15.5 nm), and CdSe ($\Delta d_h$ = 7 nm).

Transmission electron microscopy (TEM) allows for structural information on the formed CP-NP nanohybrids to be obtained. Samples were drop cast onto holey carbon copper TEM grids from THF and allowed to dry before imaging. It can be seen that no change in the shape or size of the NPs occurs post-functionalization with **2** (Figure 2a,b and c,d). Interestingly, it can be seen that, upon drying, the polymer-coated NPs **3b** and **4b** (see Figure 2b and the Supporting Information) were shown to spontaneously assemble into polymer films embedded with NPs, confirmed by scanning electron microscopy (SEM; see Supporting Information). In the CdSe CP−NP nanohybrid system it can be seen that the polymer-coated NPs (**5b**) assemble into spherical agglomerates (Figure 2d), an observation that is confirmed by AFM (vide infra). These effects are not observed with unfunctionalized NPs, which are shown to either aggregate or remain isolated from neighboring NPs (Figure 2a). Despite differences in the macroscale assembly of the CP−NP nanohybrids, it is important to note that, on account of the direct covalent attachment of **2** to the NPs, macrophase separation of the NPs from the CPs is never observed. These polymer-coated NPs can provide high interfacial surface areas between the two components, leading to well-constructed *p*−*n* heterojunctions, allowing for the rapid separation of excitons into holes and electrons and potentially yielding devices with high QEs, electronic pathways, and long lifetimes.

Topographical measurements taken by AFM reveal more about the macroscale assembly of the CP−NP nanohybrids. Prior to analysis, samples were drop-cast from either THF or toluene onto freshly cleaved mica surfaces. Images were taken in either noncontact mode for CdSe QDs or contact mode for the Au and AgNPs, using an 80 μm scanner. Comparing AFM


DOI: 10.1021/mz500645c
ACS Macro Lett. 2015, 4, 255−259

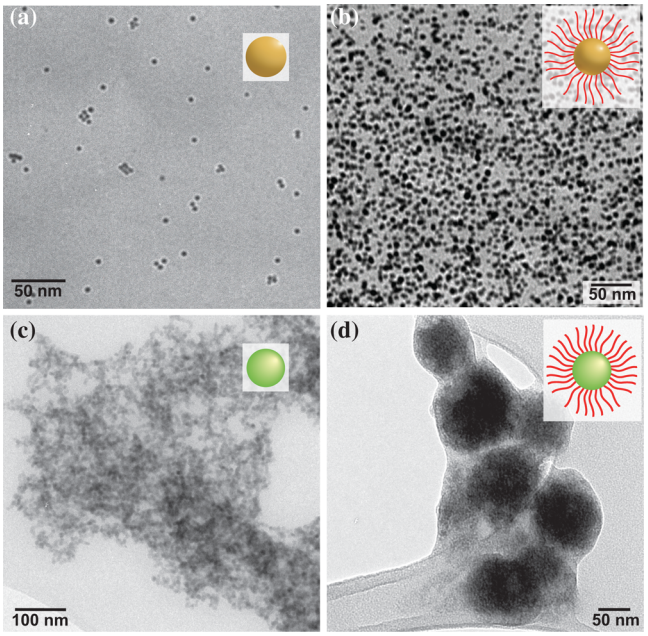


**Figure 2.** High resolution TEM images of (a) Au–NP **3a**, (b) Au CP–NP nanohybrid **3b**, (c) CdSe–NP **5a**, and (d) CdSe CP–NP nanohybrid **5b**.

images of **3a** and **3b** (Figure 3a and b, respectively), a clear change in assembly behavior can be seen. While **3a** shows

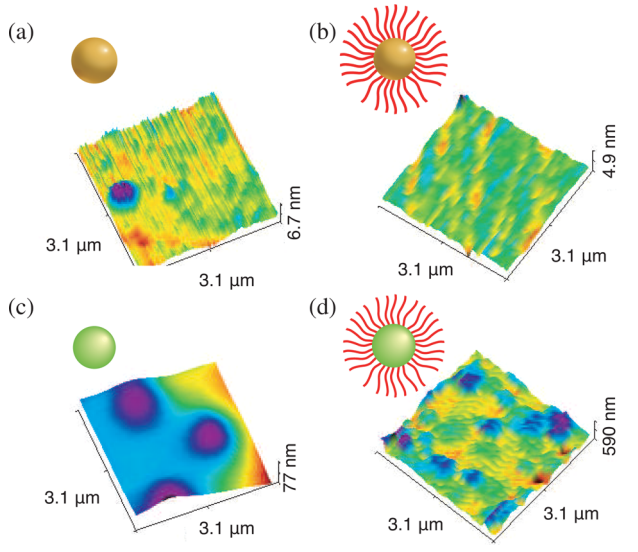


**Figure 3.** AFM topographical measurements of (a) Au–NP **3a**, (b) Au CP–NP hybrid **3b**, (c) CdSe–NP **5a**, (d) CdSe CP–NP nanohybrid **5b**.

discrete NPs, validated by TEM above, **3b** shows a rough film, likely formed by close packing of the CP–NP nanohyrids. A similar observation can be made for **4a** and **4b**; however, in the case of **4b**, the film appears much smoother than that seen for **3b**, with surface roughness of just 1.9 nm compared to 4.9 nm for **3b** (see Supporting Information). In agreement with the TEM images of the CdSe CP–NP nanohybrids, **5a** appears to aggregate upon drying to give structures in the region of 77 nm in size (Figure 3c). The same behavior is observed for **5b** (Figure 3d); however, the aggregate size is significantly increased, confirming the assembly of macroscale agglomerates of CdSe CP–NPs shown in the TEM images (Figure 2d). In all cases, the CP–NP nanohybrids appear to form larger structures than the NPs alone, likely on account of the propensity for CP self-assembly.

Utilizing RAFT polymerization, we have demonstrated the ability to synthesize a HT polymer and its subsequent rapid reduction with hydrazine to afford thiol-terminated Z group polymers, which have been fully characterized by NMR and GPC. Postpolymerization functionalization allows for the facile covalent tethering of polymer **2** to Au, Ag, and CdSe NPs to produce covalent CP–NP nanohybrids. The formation of these CP–NP nanohybrids was confirmed by UV–vis, DLS, TEM, AFM, and GPC. The CP–NP nanohybrids displayed broad spectral absorbances that ranged from the UV through visible to the near-IR and their facile synthesis and purification may allow for industrial scale up making them potentially important materials for optoelectronic device applications. Device fabrication, analyses, and potential application are currently being investigated.

## ■ ASSOCIATED CONTENT

### Supporting Information

$^1$H NMR, GPC, DLS, and experimental procedures. This material is available free of charge via the Internet at http://pubs.acs.org.

## ■ AUTHOR INFORMATION

### Corresponding Author

*E-mail: oas23@cam.ac.uk.

### Author Contributions

†P.E.W. and S.T.J. contributed equally to this work.

### Notes

The authors declare no competing financial interest.

## ■ ACKNOWLEDGMENTS

E.A.A. thanks Schlumberger for financial support. This work was supported in part by Atomic Weapons Establishment (AWE), the Walters-Kundert foundation, and an ERC Starting Investigator Grant (ASPiRe, 240629).

## ■ REFERENCES

(1) Lin, Z. *Chem.—Eur. J.* **2008**, *14*, 6294–6301.
(2) Xu, J.; Xia, J.; Lin, Z. *Angew. Chem.* **2007**, *119*, 1892–1895.
(3) Xu, J.; Xia, J. F.; Wang, J.; Shinar, J.; Lin, Z. Q. *Appl. Phys. Lett.* **2006**, *89*, 133110.
(4) Sih, B. C.; Wolf, M. O. *Chem. Commun.* **2005**, 3375–3384.
(5) Mehata, M. S. *Appl. Phys. Lett.* **2012**, *100*, 151908.
(6) Schwartz, B. J. *Annu. Rev. Phys. Chem.* **2003**, *54*, 141–172.
(7) Xu, J.; Xia, J. F.; Hong, S. W.; Lin, Z. Q.; Qiu, F.; Yang, Y. L. *Phys. Rev. Lett.* **2006**, *96*, 066104.
(8) Skaff, H.; Sill, K.; Emrick, T. *J. Am. Chem. Soc.* **2004**, *126*, 11322–11325.
(9) Odoi, M. Y.; Hammer, N. I.; Sill, K.; Emrick, T.; Barnes, M. D. *J. Am. Chem. Soc.* **2006**, *128*, 3506–3507.
(10) Milliron, D. J.; Alivisatos, A. P.; Pitois, C.; Edder, C.; Fréchet, J. M. J. *Adv. Mater.* **2003**, *15*, 58–61.
(11) Milliron, D. J.; Gur, I.; Alivisatos, A. P. *MRS Bull.* **2005**, *30*, 41–44.
(12) Liang, Z.; Dzienis, K. L.; Xu, J.; Wang, Q. *Adv. Funct. Mater.* **2006**, *16*, 542–548.
(13) Xu, J.; Wang, J.; Mitchell, M.; Mukherjee, P.; Jeffries-El, M.; Petrich, J. W.; Lin, Z. Q. *J. Am. Chem. Soc.* **2007**, *129*, 12828–12833.
(14) Friend, R. H.; Denton, G. J.; Halls, J. J. M.; Harrison, N. T.; Holmes, A. B.; Kohler, A.; Lux, A.; Moratti, S. C.; Pichler, K.; Tessler,



DOI: 10.1021/mz500645c
*ACS Macro Lett.* 2015, 4, 255–259

N.; Towns, K.; Wittmann, H. F. *Solid State Commun.* **1997**, *102*, 249−258.
(15) Bozano, L.; Carter, S. A.; Scott, J. C.; Malliaras, G. G.; Brock, P. J. *Appl. Phys. Lett.* **1999**, *74*, 1132−1134.
(16) Arango, A. C.; Johnson, L. R.; Bliznyuk, V. N.; Schlesinger, Z.; Carter, S. A.; Hörhold, H. H. *Adv. Mater.* **2000**, *12*, 1689−1692.
(17) Gur, I.; Fromer, N. A.; Chen, C. P.; Kanaras, A. G.; Alivisatos, A. P. *Nano Lett.* **2007**, *7*, 409−414.
(18) Huynh, W. U.; Dittmer, J. J.; Libby, W. C.; Whiting, G. L.; Alivisatos, A. P. *Adv. Funct. Mater.* **2003**, *13*, 73−79.
(19) Querner, C.; Benedetto, A.; Demadrille, R.; Rannou, P.; Reiss, P. *Chem. Mater.* **2006**, *18*, 4817−4826.
(20) Locklin, J.; Patton, D.; Deng, S. X.; Baba, A.; Millan, M.; Advincula, R. C. *Chem. Mater.* **2004**, *16*, 5187−5193.
(21) Advincula, R. C. *Dalton Trans.* **2006**, 2778−2784.
(22) Zhang, Q. L.; Russell, T. P.; Emrick, T. *Chem. Mater.* **2007**, *19*, 3712−3716.
(23) Querner, C.; Reiss, P.; Bleuse, J.; Pron, A. *J. Am. Chem. Soc.* **2004**, *126*, 11574−11582.
(24) Querner, C.; Reiss, P.; Zagorska, M.; Renault, O.; Payerne, R.; Genoud, F.; Rannou, P.; Pron, A. *J. Mater. Chem.* **2005**, *15*, 554−563.
(25) Querner, C.; Reiss, P.; Sadki, S.; Zagorska, M.; Pron, A. *Phys. Chem. Chem. Phys.* **2005**, *7*, 3204−3209.
(26) Antoun, T.; Brayner, R.; Al terary, S.; Fiévet, F.; Chehimi, M.; Yassar, A. *Eur. J. Org. Chem.* **2007**, *2007*, 1275−1284.
(27) Qi, X.-Y.; Pu, K.-Y.; Fang, C.; Wen, G.-A.; Zhang, H.; Boey, F. Y. C.; Fan, Q.-L.; Wang, L.-H.; Huang, W. *Macromol. Chem. Phys.* **2007**, *208*, 2007−2017.
(28) De Girolamo, J.; Reiss, P.; Pron, A. *J. Phys. Chem. C* **2007**, *111*, 14681−14688.
(29) Schenning, A. P. H. J.; Meijer, E. W. *Chem. Commun.* **2005**, 3245−3258.
(30) Williams, P. E.; Moughton, A. O.; Patterson, J. P.; Khodabakhsh, S.; O'Reilly, R. K. *Polym. Chem.* **2011**, *2*, 720−729.
(31) Moad, G.; Chen, M.; Haussler, M.; Postma, A.; Rizzardo, E.; Thang, S. H. *Polym. Chem.* **2011**, *2*, 492−519.
(32) Moad, G.; Rizzardo, E.; Thang, S. H. *Polymer* **2008**, *49*, 1079−1131.
(33) Keddie, D. J.; Moad, G.; Rizzardo, E.; Thang, S. H. *Macromolecules* **2012**, *45*, 5321−5342.
(34) Schue, F. *Polym. Int.* **2002**, *51*, 370.
(35) Moad, G.; Rizzardo, E.; Thang, S. H. *Polym. Int.* **2011**, *60*, 9−25.
(36) Lowe, A. B.; Sumerlin, B. S.; Donovan, M. S.; McCormick, C. L. *J. Am. Chem. Soc.* **2002**, *124*, 11562−11563.
(37) Shen, W.; Qiu, Q.; Wang, Y.; Miao, M.; Li, B.; Zhang, T.; Cao, A.; An, Z. *Macromol. Rapid Commun.* **2010**, *31*, 1444−1448.
(38) Noh, J. *Bull. Korean Chem. Soc.* **2005**, *26*, 553.
(39) Klajn, R.; Fang, L.; Coskun, A.; Olson, M. A.; Wesson, P. J.; Stoddart, J. F.; Grzybowski, B. A. *J. Am. Chem. Soc.* **2009**, *131*, 4233−4235.
(40) Klajn, R.; Stoddart, J. F.; Grzybowski, B. A. *Chem. Soc. Rev.* **2010**, *39*, 2203−2237.
(41) Daniel, M.-C.; Astruc, D. *Chem. Rev.* **2003**, *104*, 293−346.
(42) Schmid, G.; Baumle, M.; Geerkens, M.; Heim, I.; Osemann, C.; Sawitowski, T. *Chem. Soc. Rev.* **1999**, *28*, 179−185.
(43) Alivisatos, A. P. *Science* **1996**, *271*, 933−937.
(44) Peng, X.; Wilson, T. E.; Alivisatos, A. P.; Schultz, P. G. *Angew. Chem.* **1997**, *109*, 113−115.
(45) Many thanks to Mr. Rene Kist and Prof. Sir Richard Friend for donating the quantum dots used in this research.



DOI: 10.1021/mz500645c
*ACS Macro Lett.* 2015, 4, 255−259